JACS
JOURNAL OF THE AMERICAN CHEMICAL SOCIETY
Article
pubs.acs.org/JACS

Emergent Ion-Gated Binding of Cationic Host–Guest Complexes within Cationic $M_{12}L_{24}$ Molecular Flasks

Carson J. Bruns,[†,‡] Daishi Fujita,[§,‡] Manabu Hoshino,[§] Sota Sato,[§] J. Fraser Stoddart,*[,†] and Makoto Fujita*[,§]

[†]Department of Chemistry, Northwestern University, 2145 Sheridan Road, Evanston, Illinois 60201-3113, United States
[§]Department of Applied Chemistry, School of Engineering, The University of Tokyo, 7-3-1 Hongo, Bunkyo-ku, Tokyo 113-8656, Japan

Supporting Information

ABSTRACT: "Molecular flasks" are well-defined supramolecular cages that can encapsulate one or more molecular guests within their cavities and, in so doing, change the physical properties and reactivities of the guests. Although molecular flasks are powerful tools for manipulating matter on the nanoscale, most of them are limited in their scope because of size restrictions. Recently, however, increasingly large and diverse supramolecular cages have become available with enough space in their cavities for larger chemical systems such as polymers, nanoparticles, and biomolecules. Here we report how a class of metallosupramolecular cages known as $M_{12}L_{24}$ polyhedra have been adapted to serve as nanometer-scale containers for solutions of a pseudorotaxane host–guest complex based on a tetracationic cyclophane host, cyclobis(paraquat-*p*-phenylene) ($CBPQT^{4+}$), and a 1,5-dioxynaphthalene (DNP) guest. Remarkably, the hierarchical integration of pseudorotaxanes and $M_{12}L_{24}$ superhosts causes the system to express stimulus-responsive behavior, a property which can be described as emergent because neither the DNP⊂$CBPQT^{4+}$ nor the $M_{12}L_{24}$ assemblies exhibit this behavior independently. The DNP-containing $M_{12}L_{24}$ molecular flasks are effectively "sealed off" to $CBPQT^{4+}$ until ions are added as a stimulus to "open" them. The electrolyte stimulus reduces the electrostatic screening distance in solution, allowing favorable DNP⊂$CBPQT^{4+}$ host–guest interactions to overcome repulsive Coulombic interactions between the cationic $M_{12}L_{24}$ cages and $CBPQT^{4+}$ rings. This unusual example of ion-gated transport into chemical nanocontainers is reminiscent of transmembrane ion channels which act as gates to the cell, with the important difference that this system is reversible and operates at equilibrium.

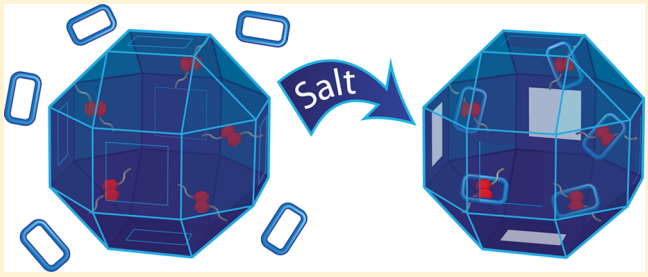

INTRODUCTION

The properties and reactivities of molecules contained within the well-defined cavities of self-assembled molecular flasks often deviate significantly from what is observed in bulk because the steric and electrostatic properties of the container become important parameters in a nanoscale size regime.[1] The recent advent of relatively large self-assembled cages[2] and metallacages[3] has created new opportunities to investigate larger systems in these confined nanospaces. Giant hollow M_nL_{2n} spherical complexes[4] such as $M_{12}L_{24}$[5] and $M_{24}L_{48}$[6] assemblies have already served as hosts for inorganic nanoparticles,[7] proteins,[8] polymers,[9] dendrimers,[10] and supramolecular assemblies,[11] for which there were previously no available molecular flasks with sufficiently large volumes. We were motivated to orchestrate the hierarchical[12] self-assembly of host–guest complexes within $M_{12}L_{24}$ molecular flasks to investigate the effects of nanoscale confinement on host–guest[13] chemistry. One type of host–guest complex that has been utilized in several integrated systems[14] of technological interest comprises a tetracationic cyclophane host, cyclobis(paraquat-*p*-phenylene) ($CBPQT^{4+}$), and π-electron-rich aromatic guests such as 1,5-dioxynaphthalene (DNP) derivatives. These components form stable pseudorotaxanes, supported by weak, non-covalent bonds such as [C–H···O], [C–H···π], π–π, and charge-transfer (CT) interactions.[15] Since both $CBPQT^{4+}$ rings and $M_{12}L_{24}$ molecular flasks are multicationic, we also anticipated showcasing the power of these weak non-covalent bonding interactions by developing a rational strategy for stabilizing the enclathration of cationic guests by the cationic hosts.[16] Here, we demonstrate that encapsulation of $CBPQT^{4+}$ rings by cationic $M_{12}L_{24}$ flasks charged with endohedral DNP units can be realized in solution only after salt has been added as a stimulus, and we suggest that the increased ionic strength is essential for screening repulsive Coulombic forces between the $CBPQT^{4+}$ rings and the $M_{12}L_{24}$ containers. The shell of the $M_{12}L_{24}$ flask thus plays the same role in this system as transmembrane ion channels play in biology,[17] acting as a gate that is bypassed only in response to an applied stimulus.

Received: May 30, 2014
Published: July 21, 2014

   dx.doi.org/10.1021/ja505296e | J. Am. Chem. Soc. 2014, 136, 12027–12034

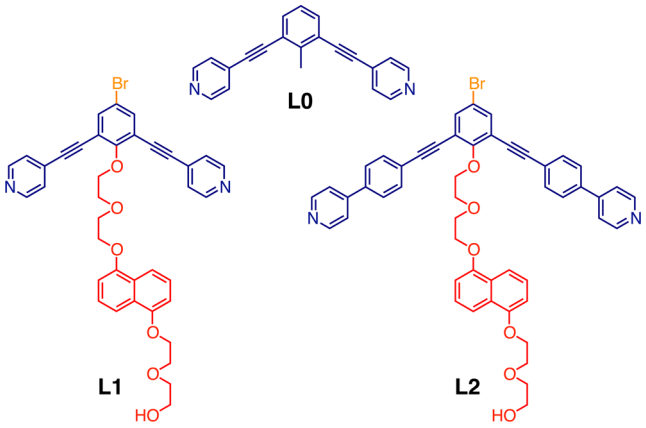

Figure 1. Structural formulas of ligands **L0**, **L1**, and **L2**.

RESULTS AND DISCUSSION

The $M_{12}L_{24}$ precursor ligands (**L0**, **L1**, and **L2**) used in this study are listed in Figure 1. The different sizes and functionalities of these ligands offer control over the volume and internal DNP concentration of the corresponding molecular flasks. Ligands **L1** and **L2** were synthesized by Sonogashira cross-coupling of alkyne-functionalized pyridines with a DNP-functionalized 4-bromo-2,6-diiodophenol [see section S2 of the Supporting Information (SI)]. These ligands were designed so as to direct their polyether-functionalized DNP recognition units (red in Figure 1) into the hollow cavities of the corresponding $M_{12}L_{24}$ molecular flasks, while displaying heavy bromine atoms exohedrally to improve X-ray crystallographic resolution in the solid state. Ligand **L0** has been previously incorporated[18] into $M_{12}L_{24}$ assemblies and was chosen because its backbone is isostructural with **L1** without having an appended DNP unit. Thus $M_{12}L_{24}$ assemblies constituting mixtures of **L0** and **L1** will create "empty" sites within the corresponding $M_{12}L_{24}$ molecular flasks, allowing us to compare the properties of the DNP⊂CBPQT^{4+} host–guest complexes in isovolumetric molecular flasks with different internal concentrations of DNP units. **L2** has an extended ligand backbone compared to **L0** and **L1** and so results in the formation of more voluminous molecular flasks.

We first characterized the **L1**⊂CBPQT^{4+} pseudorotaxane (Figure 2). Association constants (Figure 2a) were determined by isothermal titration calorimetry[19] (ITC) in DMF (K_a = 257 ± 8 M^{-1}), Me_2CO (K_a = 882 ± 112 M^{-1}), MeCN (K_a = 5855 ± 824 M^{-1}), and 1:1 Me_2SO:MeCN (K_a = 1333 ± 110 M^{-1}) at 25 °C (section S9 of the SI). We obtained higher association constants using nonlinear least-squares curve fitting of spectrophotometric titrations (section S3 of the SI), monitoring the growth of a characteristic CT absorption band at λ = 530 nm in DMF (K_a = 850 ± 70 M^{-1}), Me_2SO (K_a = 1290 ± 40 M^{-1}), and MeCN (K_a = (6.0 ± 1.1) × 10^4 M^{-1}). In spite of the fact that **L1**⊂CBPQT^{4+} is most weakly associated in DMF, we used DMF-d_7 for NMR spectroscopy (Figure 2b–d) because of its low freezing temperature. At room temperature, the ^{1}H signals of **L1**⊂CBPQT^{4+} are very broad (Figure 2c) in all of the selected solvent systems because of an intermediate rate of exchange between complexed and uncomplexed components on the ^{1}H NMR time scale. In particular, the 3/

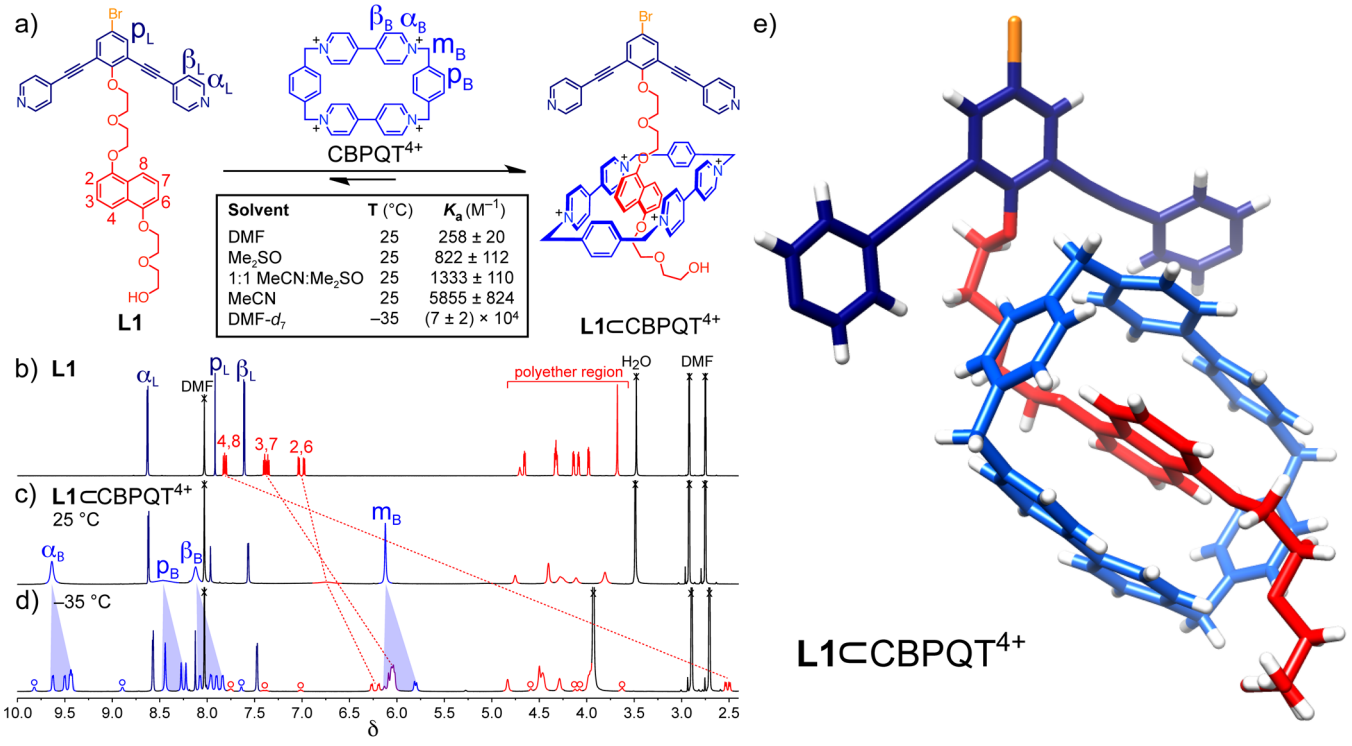

Figure 2. Characterization of the **L1**⊂CBPQT^{4+} host–guest complex. (a) Self-assembly of the **L1**⊂CBPQT^{4+} host–guest complex and association constants in selected solvents. (b–d) Comparison of the ^{1}H NMR spectra (DMF-d_7, 600 MHz) of (b) **L1** at 25 °C, (c) **L1**⊂CBPQT^{4+} at 25 °C, and (d) **L1**⊂CBPQT^{4+} at −35 °C. An intermediate exchange rate at 25 °C broadens the signals in (b), especially for the 3/7 and 4/8 DNP protons which are unobservable. At −35 °C, exchange is slow on the NMR time scale, and the uncomplexed **L1** (red, dark blue) and CBPQT^{4+} (blue) signals (designated by open circles) can be identified in addition to the dominant signals of the **L1**⊂CBPQT^{4+} complex. (e) Solid-state structure of **L1**⊂CBPQT·4PF_6 (solvent molecules and counterions omitted for clarity).

dx.doi.org/10.1021/ja505296e | J. Am. Chem. Soc. 2014, 136, 12027–12034

7 and 4/8 DNP protons are so highly shielded by CBPQT^{4+} that extensive line broadening renders the corresponding signals unobservable. At low temperatures, the system transitions to a slow exchange regime in which well-resolved signals of both complexed and uncomplexed species can be observed (Figure 2d) and assigned. Thus we determined (Figure S4) an association constant for **L1**⊂CBPQT^{4+} in DMF ($K_a = (7 \pm 2) \times 10^4$ M^{-1}) at −35 °C using the ^{1}H NMR single-point analysis method.[20] Single crystals suitable for X-ray analysis were grown by slow vapor diffusion of ^{i}Pr$_2$O into a solution of **L1**⊂CBPQT·4PF$_6$ in MeCN (section S6 of the SI). The solid-state structure of the host−guest complex is shown in Figure 2e. The DNP⊂CBPQT^{4+} host−guest complex is endotopic with respect to the divalent ligand moiety. No significant interactions between the ligand backbone and the DNP⊂CBPQT^{4+} pseudorotaxane are observed, suggesting to us that the orthogonal self-assembly of the $M_{12}L_{24}$ cages and the host−guest complexes would be possible.

The self-assembly of a **Pd$_{12}$L1$_{24}$**$^{24+}$ coordination sphere (Figure 3a) has been achieved by treating ligand **L1** with 0.5 equiv of Pd(BF$_4$)$_2$ for 1 h at 60 °C in polar organic solvents, such as MeCN, Me$_2$SO, and DMF. Single crystals suitable for X-ray crystallographic analysis were grown by slow vapor diffusion of EtOAc into a solution of **Pd$_{12}$L1$_{24}$**·24BF$_4$ in Me$_2$SO (Figure 3b; see section S6 of the SI). The endohedral DNP threads are disordered within the cage assemblies, allowing us to resolve only a few of the polyether atoms near the ligand backbone. The close packing in the X-ray crystal superstructure (Figure 3c) shows that there is insufficient space between the $M_{12}L_{24}$ assemblies for DNP units to occupy, suggesting that the threads are fully contained within the internal cavities of these molecular flasks.

Pd$_{12}$L0$_{12}$L1$_{12}$ $^{24+}$ and **Pd$_{12}$L2$_{24}$**$^{24+}$ assemblies were prepared in the same manner as **Pd$_{12}$L1$_{24}$**$^{24+}$. In order to assess the dimensionality and volume of the molecular flasks with respect to the CBPQT^{4+} host, DNP threads were modeled within the crystallographically determined structures of **Pd$_{12}$L1$_{24}$**$^{24+}$ and previously reported[11,21] $Pd_{12}L_{24}$ cages with ligand backbone motifs that are isostructural with those of **Pd$_{12}$L0$_{12}$L1$_{12}$**$^{24+}$ and **Pd$_{12}$L2$_{24}$**$^{24+}$. The geometries of the DNP threads were optimized by molecular mechanics using the MM+ force field. Table 1 summarizes the cage dimensions and volumes from this analysis. The total volumes of the molecular flasks are defined by the outermost atoms on the central phenylene units of the ligands, which constitute the vertices of a rhombicuboctahedron. Although **Pd$_{12}$L1$_{24}$**$^{24+}$ encloses a large 44.4 nm^3 volume of space, 17.5 nm^3 (~43%) of this space is occupied by the ligands and 12 endohedral BF$_4^-$ counterions. Ignoring electrostatic limitations, this analysis indicates that 11 CBPQT^{4+} rings—each at a volume of 0.66 nm^3, including four BF$_4^-$ counterions—can fill the sphere's cavity at any one time, taking Rebek's 55% solution[22] for the packing coefficient in liquids to be the upper limit, whereas up to 21 CBPQT^{4+} rings can be accommodated at the 70% solution for systems with strong intermolecular forces.[22] **Pd$_{12}$L0$_{12}$L1$_{12}$**$^{24+}$ can accommodate CBPQT^{4+} hosts on all 12 of its endohedral threads by the same analysis. **Pd$_{12}$L2$_{24}$**$^{24+}$ also has enough space for CBPQT^{4+} to occupy all 24 of its endohedral threads, with its capacious 107 nm^3 of free volume on the basis of sterics alone. The diameter of the cages' openings in comparison with the cross-section of CBPQT^{4+} is another important consideration. The $M_{12}L_{24}$ spheres have two sets of apertures: six square pores comprising four Pd^{2+} corners bridged by four ligands, and eight triangular pores comprising three Pd^{2+} corners bridged by three ligands. We conclude that these windows are large enough for the CBPQT^{4+} rings to pass through—e.g., the 1.8 × 1.8 nm^2 pore of the smaller **Pd$_{12}$L1$_{24}$**$^{24+}$ sphere is much larger than even the widest dimensions of CBPQT^{4+} at 1.1 × 0.65 nm^2.

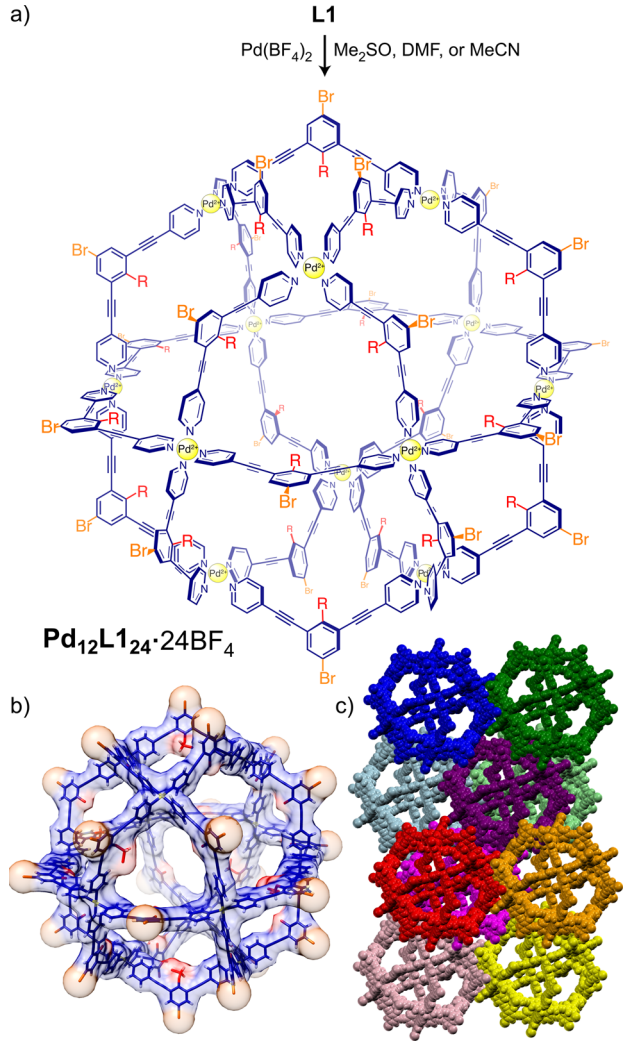

Figure 3. Structure of **Pd$_{12}$L1$_{24}$**$^{24+}$. (a) Self-assembly of **Pd$_{12}$L1$_{24}$**·24BF$_4$ from ligand **L1** and Pd(BF$_4$)$_2$·4MeCN in polar organic solvents. (b) Solid-state structure of **Pd$_{12}$L1$_{24}$**·24BF$_4$. Disordered sites and BF$_4^-$ counterions are omitted for clarity. (c) Solid-state superstructure of **Pd$_{12}$L1$_{24}$**·24BF$_4$. The close packing of the **Pd$_{12}$L1$_{24}$**$^{24+}$ assemblies provides insufficient interstitial space for DNP units, indicating that the DNP threads are contained within the molecular flasks.

We further confirmed the assembly of the molecular flasks using cold-spray ionization mass spectrometry (Figures S12 and S13). With parent molecular weights of 19 971 and 23 620 Da respectively, the ions $[M - nBF_4]^{n+}$ were observed, where n = 7−16 for **Pd$_{12}$L1$_{24}$**$^{24+}$ (Figure S12a) and n = 8−18 for **Pd$_{12}$L2$_{24}$**$^{24+}$ (Figure S12b). The mass spectrum of the mixed-ligand **Pd$_{12}$L0$_{12}$L1$_{12}$**·24BF$_4$ molecular flasks (Figure S13), on the other hand, indicates the existence of a statistical mixture of cages with different **L0**:**L1** ratios, where the 1:1 molar ratio is an average value.

Pd$_{12}$L1$_{24}$ $^{24+}$ and **Pd$_{12}$L2$_{24}$**$^{24+}$ were characterized in solution by ^{1}H and ^{13}C NMR spectroscopy (Figures S5−S8) and also ^{1}H DOSY NMR spectroscopy (Figures S9 and S10), which

dx.doi.org/10.1021/ja505296e | J. Am. Chem. Soc. 2014, 136, 12027−12034

Table 1. Dimensions and Volumes of $Pd_{12}L_{24}$ Molecular Flasks, Determined by Modeling the Endohedral DNP Threads within the Solid-State Structures of the Corresponding Metallosupramolecular Polyhedra

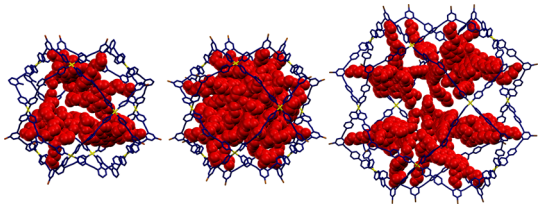

	$Pd_{12}L0_{12}L1_{12}$	$Pd_{12}L1_{24}$	$Pd_{12}L2_{24}$
average radius[a]	2.31 nm	2.35 nm	3.16 nm
total volume	43.4 nm^3	44.4 nm^3	128 nm^3
occupied volume	12.3 nm^3	17.5 nm^3	21.1 nm^3
percentage occupied	28%	39%	16%
aperture width[b]	1.8 nm	1.8 nm	2.3 nm

[a]Average Br−centroid distance. [b]Minimum edge width of the larger square pores of the $Pd_{12}L_{24}$ structure.

verified their quantitative assembly. The ^{1}H NMR spectra each show a single set of signals with downfield shifts of the ligand's α and β proton resonances and line broadening that are characteristic of $Pd_{12}L_{24}$ assemblies, as well a single diffusion band in the ^{1}H DOSY NMR spectra. $\mathbf{Pd_{12}L1_{24}}^{24+}$ and $\mathbf{Pd_{12}L2_{24}}^{24+}$ diffuse almost an order of magnitude slower [$(1.1 \pm 0.2) \times 10^{-10}$ and $(6.6 \pm 0.8) \times 10^{-11}$ m^2 s^{-1}, respectively] than their parent ligands **L1** and **L2** [$(4.6 \pm 0.5) \times 10^{-10}$ and $(4.2 \pm 0.6) \times 10^{-10}$ m^2 s^{-1}, respectively] in DMF-d_7. Figure 4 compares the aromatic signals in the ^{1}H NMR

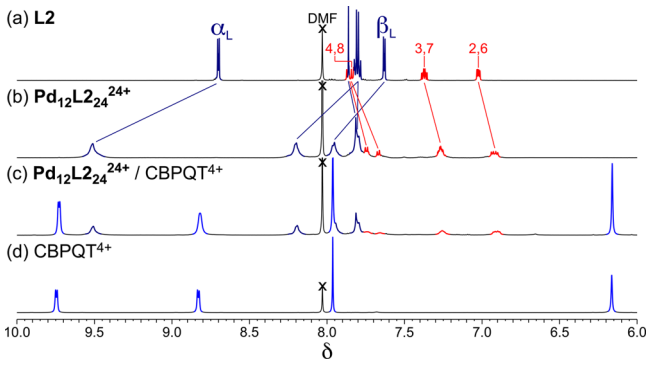

Figure 4. Comparison of the partial ^{1}H NMR spectra (600 MHz, DMF-d_7, 298 K) of (a) **L2**, (b) $\mathbf{Pd_{12}L2_{24}}^{24+}$, (c) a $\mathbf{Pd_{12}L2_{24}}^{24+}$ and $CBPQT^{4+}$ mixture, and (d) $CBPQT^{4+}$.

spectra of (a) **L2**, (b) $\mathbf{Pd_{12}L2_{24}}^{24+}$, (c) $CBPQT^{4+}$ with a 1:24 mixture of $\mathbf{Pd_{12}L2_{24}}^{24+}$, and (d) $CBPQT^{4+}$ in DMF-d_7. In contrast with the unencapsulated DNP⊂$CBPQT^{4+}$ complex (Figure 2c), no significant shifting or broadening of the DNP and $CBPQT^{4+}$ proton signals is observed in the $\mathbf{Pd_{12}L2_{24}}^{24+}$−$CBPQT^{4+}$ mixture. The same behavior was observed for $\mathbf{Pd_{12}L1_{24}}^{24+}$. The ^{1}H DOSY NMR spectrum of the $\mathbf{Pd_{12}L2_{24}}^{24+}$−$CBPQT^{4+}$ mixture (Figure S11) shows two separate diffusion bands for the cage and $CBPQT^{4+}$, with diffusion rates that are almost identical to those observed in the unmixed components. Furthermore, the expected CT absorption band near 530 nm is not observed for either $Pd_{12}L_{24}$−$CBPQT^{4+}$ mixture. These data all point to a complete lack of interaction between the $CBPQT^{4+}$ rings and the endohedral DNP threads of the molecular flasks. Since molecular models indicate that $CBPQT^{4+}$ is not forbidden to enter the cages by steric constraints, it follows that repulsion between the 24 positive charges of the $Pd_{12}L_{24}$ cages and the four pyridinium cations of the $CBPQT^{4+}$ rings creates an electrostatic barrier that is responsible for excluding the molecular hosts ($CBPQT^{4+}$) from the superhost ($Pd_{12}L_{24}$ assemblies) in solution.

Although the molecular flasks are "sealed off" to $CBPQT^{4+}$ in neat solvents, the apertures of the $Pd_{12}L_{24}$ assemblies are on the same length scale as the Bjerrum length (distance at which the magnitude of electrostatic interactions is equal to that of the thermal energy, k_BT), which is approximately 1.2 nm in Me_2SO. We therefore reasoned that increasing the ionic strength of the solution could lower the Coulombic barrier between the $Pd_{12}L_{24}$ and $CBPQT^{4+}$ macrocations by screening their repulsive interactions so as to "open" the molecular flasks. It has been established[23] that $M_{12}L_{24}$ cages can assemble into much larger aggregates that gradually precipitate irreversibly in a process that is accelerated in solutions of greater ionic strength. We therefore optimized the solvent and ion compositions and concentrations in order to avoid precipitation of the molecular flasks. We found that tetrabutylammonium salts with soft counteranions (e.g., NBu_4BF_4, NBu_4PF_6) effectively stabilize the $\mathbf{Pd_{12}L1_{24}}^{24+}$ assemblies in Me_2SO. Electrolytes with harder anions (e.g., NBu_4NO_3, NBu_4Br) or alkali metals (e.g., $NaBF_4$, KPF_6) cause $\mathbf{Pd_{12}L1_{24}}^{24+}$ to precipitate rapidly, as do alternative solvents such as MeCN and DMF. Thus Me_2SO was the only solvent in which precipitation of $\mathbf{Pd_{12}L1_{24}}^{24+}$ could be avoided across all practical concentrations of NBu_4BF_4. Unfortunately, $\mathbf{Pd_{12}L2_{24}}^{24+}$ begins to precipitate in all solvents even at relatively low concentrations (<100 mM) of any of these electrolytes.

The order of addition plays a nontrivial role in the DNP⊂$CBPQT^{4+}$⊂$Pd_{12}L_{24}{}^{24+}$ systems. Precipitation of the $Pd_{12}L_{24}$ assemblies can be mitigated substantially when $CBPQT^{4+}$ is added in solution prior to the electrolyte. For example, a ∼40 μM solution of $\mathbf{Pd_{12}L1_{24}}^{24+}$ (1 mM with respect to the total ligand concentration) precipitates completely in MeCN at a concentration of 100 mM NBu_4BF_4, but the solution is stable if $CBPQT^{4+}$ (1 equiv with respect to DNP) is added first. $\mathbf{Pd_{12}L2_{24}}^{24+}$ is insoluble in any charge-screened solution unless $CBPQT^{4+}$ is present. This stabilization effect is most likely caused by the rapid exchange of $CBPQT^{4+}$ in and out of the $Pd_{12}L_{24}$ molecular flasks at equilibrium, a process which presumably interferes with their self-aggregation. A stacked plot of the partial ^{1}H NMR spectra of a 1:24 mixture of $\mathbf{Pd_{12}L2_{24}}^{24+}$ and $CBPQT^{4+}$ (1:1 DNP:$CBPQT^{4+}$) in DMF-d_7 with increasing concentrations of electrolyte (Figure 5) supports this hypothesis. The DNP and $CBPQT^{4+}$ signals broaden and shift to lower frequencies with increasing ionic strength, corresponding to an increasing association constant for the endohedral DNP⊂$CBPQT^{4+}$ host−guest complexes. Analogous behavior was observed for the $\mathbf{Pd_{12}L1_{24}}^{24+}$ and $\mathbf{Pd_{12}L0_{12}L1_{12}}^{24+}$ molecular flasks. Importantly, these changes in the DNP and $CBPQT^{4+}$ signals occur without the signals of the ligand backbone being significantly affected, indicating that the $Pd_{12}L_{24}$ molecular flasks do not dissociate as $CBPQT^{4+}$ binds DNP. As in the **L1**⊂$CBPQT^{4+}$ complex (Figure 2c), the broad ^{1}H signals for DNP⊂$CBPQT^{4+}$ host−guest complexes within $\mathbf{Pd_{12}L2_{24}}^{24+}$ assemblies at 298 K indicate that monomers and complexes exchange at an intermediate rate on the ^{1}H NMR

dx.doi.org/10.1021/ja505296e | J. Am. Chem. Soc. 2014, 136, 12027−12034

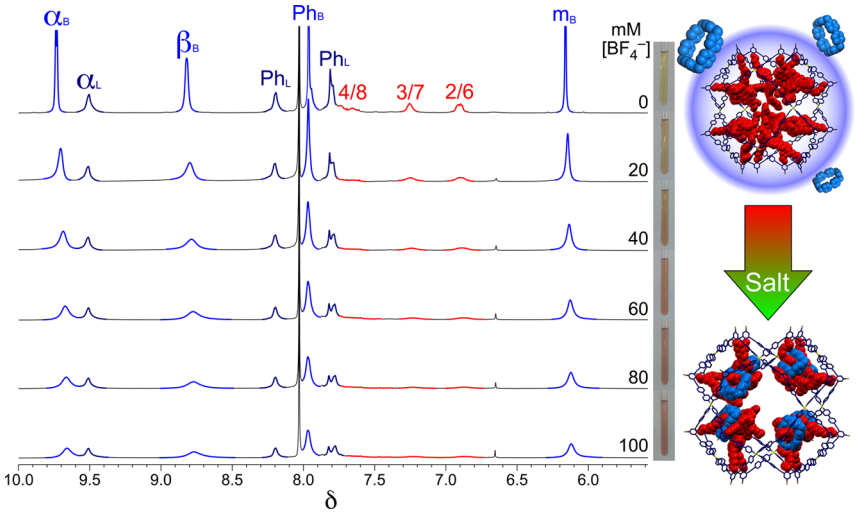

Figure 5. Stacked plot of the ^{1}H NMR spectra (600 MHz, DMF-d_7, 298 K) of a 1:1 mixture of $\mathbf{Pd_{12}L2_{24}}^{24+}$ and CBPQT^{4+} with increasing concentration of BF_4^-. Photographs of the NMR samples at right show the increasingly red color of the solution, which accompanies the broadening and disappearance of the DNP ^{1}H signals, indicating that electrolytes promote the formation of DNP⊂CBPQT^{4+} within $\mathbf{Pd_{12}L2_{24}}^{24+}$.

time scale at room temperature. Unfortunately, the broken symmetry caused by the partial introduction of CBPQT^{4+} into the flasks leads to complicated NMR spectra with many overlapping signals that we are unable to assign in the slow exchange regime at −35 °C, preventing the estimation of binding constants by ^{1}H NMR single-point analysis.

The images of the NMR samples that accompany the spectra in Figure 5 show that the addition of salt is also accompanied by changes in solution color in the direction of increasingly red hues, owing to the growth of the characteristic CT absorption attributable to the DNP⊂CBPQT^{4+} host−guest complex. Figure 6a shows the visible absorption spectra of mixtures of $\mathbf{Pd_{12}L1_{24}}^{24+}$ (1 mM with respect to total DNP concentration) and CBPQT^{4+} (5 mM) in Me_2SO at different concentrations of NBu_4BF_4. Whereas no CT absorption band is observed when $[NBu_4BF_4] = 0$, a CT band appears and grows in intensity as $[NBu_4BF_4]$ is increased. The λ_{max} of this CT band is approximately 530 nm—i.e., the same as that for **L1**⊂CBPQT^{4+}—indicating that CBPQT^{4+} rings are taken up within the molecular flasks as a consequence of hosting DNP units, rather than by side-on interactions with DNP, which absorb at significantly shorter (460−480 nm) wavelengths.[24] In order to verify that the environment of the molecular flasks does not alter the 1:1 binding stoichiometry n of the DNP⊂CBPQT^{4+} complex, we prepared a Job plot (Figure S14) of $\mathbf{Pd_{12}L1_{24}}^{24+}$ and CBPQT^{4+} in DMF with 100 mM NBu_4BF_4 electrolyte, which confirmed that n = 1 with respect to DNP in the molecular flasks. We were unable to observe the CBPQT^{4+} hosts within the $Pd_{12}L_{24}$ superhosts by mass spectrometry because the high salt concentrations needed to promote this assembly saturate the detector with cationic oligomers of NBu_4BF_4.

We used ITC (section S9 of the SI) to estimate the association constant between DNP and CBPQT^{4+} within the molecular flasks. ITC is an appropriate method for estimating K_a in low-affinity systems if the binding stoichiometry n is known.[25] All ITC experiments were carried out with respect to a total DNP concentration in solution of 1 mM. We collected a ^{1}H NMR spectrum (Figure S6) of $\mathbf{Pd_{12}L1_{24}}^{24+}$ when diluted to 1 mM with respect to DNP in CD_3SOCD_3 with 1 M NBu_4BF_4 electrolyte to confirm that the molecular flasks remain

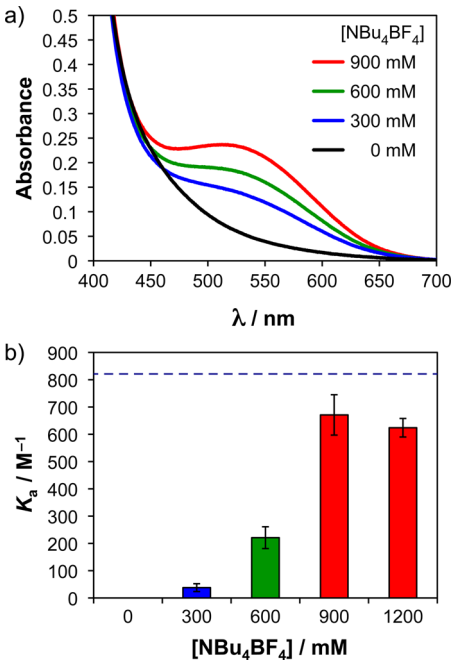

Figure 6. Characterization of the DNP⊂CBPQT^{4+} complex within $\mathbf{Pd_{12}L1_{24}}^{24+}$ molecular flasks in Me_2SO solution. (a) Comparison of the visible spectra of a mixture of $\mathbf{Pd_{12}L1_{24}}^{24+}$ (1 mM) and CBPQT^{4+} (5 equiv) at different concentrations of NBu_4BF_4, showing the appearance and increase in intensity of a characteristic CT absorption band attributable to the DNP⊂CBPQT^{4+} host−guest complex with increasing ionic strength. (b) Plot of the association constant (K_a) of DNP⊂CBPQT^{4+} (determined by ITC) in solutions of $\mathbf{Pd_{12}L1_{24}}^{24+}$ (1 mM with respect to DNP) against $[NBu_4BF_4]$. The dashed line represents the association constant of **L1**⊂CBPQT^{4+}, which is insensitive to $[NBu_4BF_4]$.

assembled under the conditions of the ITC experiments. Representative ITC data for each set of conditions are shown in section S9 of the SI. Association constants (K_a) for DNP⊂CBPQT^{4+} were determined by averaging the values obtained from nonlinear least-squares fits of the binding isotherms at a fixed value of n = 1 over three individual titration experiments. These association constants are plotted against the concen-

dx.doi.org/10.1021/ja505296e | J. Am. Chem. Soc. 2014, 136, 12027−12034

tration of NBu_4BF_4 in Figure 6b. The error margins are reported at the 95% confidence interval of twice the standard deviation over the three individual titrations for each data point. It is evident that the association of DNP⊂CBPQT^{4+} is highly sensitive to [NBu_4BF_4] within the molecular flasks. By contrast, we observed no statistical difference in K_a (shown as a dashed line in Figure 6b) of **L1**⊂CBPQT^{4+} over the same electrolyte concentration range. In a solution of $\mathbf{Pd_{12}L1_{24}}^{24+}$ with no added salt, a small, endothermic signal associated with the heat of dilution during each injection indicates no binding event (K_a = 0). The expected exothermic signal is observed in charge-screened solutions, however, and the association constant rises substantially with increasing ionic strength. The magnitude of K_a plateaus around ∼600 M^{-1} (almost 75% that of the free ligand **L1**) at NBu_4BF_4 concentrations of 900 mM and above. This association constant agrees well with the dimensional analysis (Table 1) of $\mathbf{Pd_{12}L1_{24}}^{24+}$, indicating that the flask has enough free volume for CBPQT^{4+} to occupy somewhere between 11 and 21 (46−88%) of the internal DNP sites.

In an equal mixture of Me_2SO and MeCN, the association constant for DNP⊂CBPQT^{4+} is already much higher at 100 mM NBu_4BF_4 (181 ± 50 M^{-1}) than it is at 300 mM NBu_4BF_4 in Me_2SO (38 ± 14 M^{-1}), revealing that the strength of the host−guest complex remains sensitive to solvent composition within the molecular flasks. Under these conditions, there is no statistical difference in binding affinity (Table S3) within $\mathbf{Pd_{12}L1_{24}}^{24+}$ (K_a = 181 ± 50 M^{-1}) and $\mathbf{Pd_{12}L0_{12}L1_{12}}^{24+}$ (K_a = 151 ± 68 M^{-1}), suggesting that the association constant is limited by electrostatic repulsion more than by steric crowding. Although we were unable to quantify the DNP⊂CBPQT^{4+} binding constant within the larger $\mathbf{Pd_{12}L2_{24}}^{24+}$ molecular flasks on account of their insolubility in electrolyte solutions in the absence of CBPQT^{4+}, the NMR spectroscopic results (*vide supra*) suggest similar ion-responsive behavior.

Overall, the spectroscopic and calorimetric data show that the association properties of the DNP⊂CBPQT^{4+} host−guest complex are very different inside of the nanoscale containers than they are in bulk solution. Most notably, the high sensitivity of K_a to ionic strength means that the $Pd_{12}L_{24}$ molecular flasks transform the host−guest complex into a stimulus-responsive system. This stimulus response qualifies as an emergent property, since neither the $Pd_{12}L_{24}$ nor DNP⊂CBPQT^{4+} assemblies respond to ionic stimuli independently. We note also that these assemblies are fully reversible equilibrium systems. Adding Pd^{II} to a Me_2SO solution of **L1**⊂CBPQT^{4+} causes an immediate color change from red to yellow as the assembly of $\mathbf{Pd_{12}L1_{24}}^{24+}$ expels the CBPQT^{4+} hosts from the cages. Thus, a clear hierarchy in DNP⊂CBPQT^{4+}⊂$Pd_{12}L_{24}$ is established, where the stronger $Pd_{12}L_{24}$ superhost assemblies impose on the behavior of the weaker DNP⊂CBPQT^{4+} host−guest complexes. Examples of hierarchical superhost−host−guest assemblies[26] and stimulus-gated host−guest systems[27] both remain relatively rare in the chemical literature, while this system constitutes a combination thereof.

CONCLUSIONS

We have carried out the host−guest chemistry of a cationic DNP⊂CBPQT^{4+} host−guest complex within the cavities of self-assembled, cationic $M_{12}L_{24}$ molecular flasks. The hierarchical organization of these assemblies leads to the emergence of stimulus-responsive binding properties, where the $M_{12}L_{24}$ molecular flasks are "sealed off" to the CBPQT^{4+} hosts until ions introduced in solution "open" them by screening repulsive Coulombic interactions. Thus, we have demonstrated (i) a platform for studying host−guest chemistry within molecular flasks, (ii) a rational strategy for encapsulating macrocations within macrocations, and (iii) ion-triggered binding in hierarchical self-assembled systems.

EXPERIMENTAL SECTION

General Methods. All reagents and solvents were purchased from commercial suppliers (Aldrich or TCI) and used without further purification. Nuclear magnetic resonance (NMR) spectra were recorded on Bruker Avance 500 and 600 spectrometers, with working frequencies of 500 and 600 MHz for ^{1}H, and 125 and 150 MHz for ^{13}C nuclei, respectively. Chemical shifts are reported in ppm and referenced to the residual non-deuterated solvents for ^{1}H (CD_3SOCD_3, δ = 2.50 ppm; DMF-d_7, δ = 8.03 ppm) and ^{13}C (CD_3SOCD_3, δ = 39.52 ppm; DMF-d_7, δ = 162.5 ppm). High-resolution mass spectra were recorded on either an Agilent 6210 LC-TOF electrospray ionization (ESI) mass spectrometer or a Bruker maXis instrument equipped with an automated sample injection system. Mass spectra were processed on Bruker DataAnalysis (Version 4.0 SP2) software, and the simulations were performed on Bruker IsotopePattern software. UV−visible spectral data were recorded on a Shimadzu UV-3150 spectrophotometer. Isothermal titration calorimetry was performed on a Microcal VP-ITC microcalorimeter, and the titration binding isotherms were fit in Origin 5.0 software using the standard non-interacting one-site model supplied by Microcal.

***$Pd_{12}L1_{24}$*·24BF_4.** Ligand **L1** (5.50 mg, 7.93 μmol) in DMF-d_7 (600 μL) was treated with 27 mM $Pd(BF_4)_2$ solution in DMF-d_7 (150 μL, 4.0 μmol) at 60 °C and stirred for 1 h. ^{1}H NMR (500 MHz, 298 K, DMF-d_7): δ = 9.44 (br s, 96H), 7.89 (br s, 96H), 7.82 (s, 48H), 7.63 (d, J = 8.5 Hz, 24H), 7.46 (d, J = 8.5 Hz, 24H), 7.18 (dd, J = 7.7, 8.5 Hz, 24H), 7.06 (dd, J = 7.7, 8.5 Hz, 24H), 6.87 (d, J = 7.7 Hz, 24H), 6.73 (d, J = 7.7 Hz, 24H), 4.78 (br s, 24H), 4.54 (br s, 48H), 4.24 (br s, 48H), 4.11 (br s, 48H), 3.97 (br s, 48H), 3.88 (br s, 96H), 3.70−3.64 (m, 96H). ^{13}C NMR (125 MHz, 298 K, DMF-d_7): δ = 154.6, 154.4, 151.8, 138.4, 134.9, 129.2, 126.7, 125.6, 125.5, 118.0, 117.8, 115.5, 114.4, 114.2, 106.0, 106.0, 93.0, 91.3, 75.0, 73.4, 71.1, 69.7, 69.7, 68.4, 68.0, 61.4. CSI-MS of $C_{912}H_{792}B_{24}Br_{24}F_{96}N_{48}O_{144}Pd_{12}$: m/z calcd for $C_{912}H_{792}B_{17}Br_{24}F_{68}N_{48}O_{144}Pd_{12}$ $[M-7(BF_4)]^{7+}$ 2771.224, found 2771.534; m/z calcd for $C_{912}H_{792}B_{16}Br_{24}F_{64}N_{48}O_{144}Pd_{12}$ $[M-8(BF_4)]^{8+}$ 2413.946, found 2413.973; m/z calcd for $C_{912}H_{792}B_{15}Br_{24}F_{60}N_{48}O_{144}Pd_{12}$ $[M-9(BF_4)]^{9+}$ 2136.063, found 2136.418; m/z calcd for $C_{912}H_{792}B_{14}Br_{24}F_{56}N_{48}O_{144}Pd_{12}$ $[M-10(BF_4)]^{10+}$1913.756, found 1914.077; m/z calcd for $C_{912}H_{79213}Br_{24}F_{52}N_{48}O_{144}Pd_{12}$ $[M-11(BF_4)]^{11+}$ 1731.960, found 1732.068; m/z calcd for $C_{912}H_{792}B_{12}Br_{24}F_{48}N_{48}O_{144}Pd_{12}$ $[M-12(BF_4)]^{12+}$ 1580.379, found 1580.563; m/z calcd for $C_{912}H_{792}B_{11}Br_{24}F_{44}N_{48}O_{144}Pd_{12}$ $[M-13(BF_4)]^{13+}$ 1452.119, found 1452.208; m/z calcd for $C_{912}H_{792}B_{10}Br_{24}F_{40}N_{48}O_{144}Pd_{12}$ $[M-14(BF_4)]^{14+}$ 1342.182, found 1342.261; m/z calcd for $C_{912}H_{792}B_9Br_{24}F_{36}N_{48}O_{144}Pd_{12}$ $[M-15(BF_4)]^{15+}$ 1246.903, found 1247.110; m/z calcd for $C_{912}H_{792}B_8Br_{24}F_{32}N_{48}O_{144}Pd_{12}$ $[M-16(BF_4)]^{16+}$ 1163.596, found 1162.849.

***$Pd_{12}L2_{24}$*·24BF_4.** Ligand **L2** (5.32 mg, 6.29 mmol) in DMF-d_7 (600 mL) was treated with 25 mM $Pd(BF_4)_2$ solution in DMF-d_7 (130 mL, 3.2 mmol) at 60 °C and stirred for 1 h. ^{1}H NMR (600 MHz, 298 K, DMF-d_7): d = 9.51 (br s, 96H), 8.20 (br s, 96H), 7.95 (br s, 96H), 7.81 (br s, 96H), 7.80 (s, 48H), 7.75 (d, J = 8.5 Hz, 24H), 7.67 (d, J = 8.5 Hz, 24H), 7.27 (dd, J = 7.5, 8.5 Hz, 24H), 7.26 (dd, J = 7.5, 8.5 Hz, 24H), 6.93 (d, J = 7.5 Hz, 24H), 6.91 (d, J = 7.5 Hz, 24H), 4.80 (br s, 24H), 4.63 (br s, 48H), 4.31−4.28 (m, 48H), 4.25−4.22 (m, 48H), 4.15−4.12 (m, 48H), 4.08−4.05 (m, 48H), 3.94−3.91 (m, 48H), 3.71−3.68 (m, 48H), 3.68−3.65 (m, 48H). ^{13}C NMR (125 MHz, 298 K, DMF-d_7): δ = 161.1, 154.7, 154.6, 152.1, 150.5, 135.2, 132.9, 128.0, 126.8, 126.8, 125.7, 125.6, 125.2, 124.6, 119.6, 118.0, 115.8, 114.4, 114.3, 106.2, 106.1, 94.9, 86.7, 74.5, 73.5, 71.3, 70.1, 69.8, 68.4, 68.4, 61.4. CSI-MS of $C_{1200}H_{984}B_{24}Br_{24}F_{96}N_{48}O_{144}Pd_{12}$: m/z calcd for $C_{1200}H_{984}B_{16}Br_{24}F_{64}N_{48}O_{144}Pd_{12}$ $[M-8(BF_4)]^{8+}$ 2870.510, found 2871.039; m/z calcd for $C_{1200}H_{984}B_{15}Br_{24}F_{60}N_{48}O_{144}Pd_{12}$ $[M-9(BF_4)]^{9+}$ 2541.897, found 2542.169; m/z calcd for $C_{1200}H_{984}B_{14}Br_{24}$-

dx.doi.org/10.1021/ja505296e | J. Am. Chem. Soc. 2014, 136, 12027−12034

$F_{56}N_{48}O_{144}Pd_{12}$ $[M - 10(BF_4)]^{10+}$ 2279.107, found 2279.212; *m/z* calcd for $C_{1200}H_{984}B_{13}Br_{24}F_{52}N_{48}O_{144}Pd_{12}$ $[M - 11(BF_4)]^{11+}$ 2064.006, found 2064.308; *m/z* calcd for $C_{1200}H_{984}B_{12}Br_{24}F_{48}N_{48}O_{144}Pd_{12}$ $[M - 12(BF_4)]^{12+}$ 1884.755, found 1884.702; *m/z* calcd for $C_{1200}H_{984}B_{11}Br_{24}F_{44}N_{48}O_{144}Pd_{12}$ $[M - 13(BF_4)]^{13+}$ 1733.081, found 1733.094; *m/z* calcd for $C_{1200}H_{984}B_{10}Br_{24}F_{40}N_{48}O_{144}Pd_{12}$ $[M - 14(BF_4)]^{14+}$ 1603.075, found 1603.092; *m/z* calcd for $C_{1200}H_{984}B_9Br_{24}F_{36}N_{48}O_{144}Pd_{12}$ $[M - 15(BF_4)]^{15+}$ 1490.470, found 1490.414; *m/z* calcd for $C_{1200}H_{984}B_8Br_{24}F_{32}N_{48}O_{144}Pd_{12}$ $[M - 16(BF_4)]^{16+}$ 1391.878, found 1391.824; *m/z* calcd for $C_{1200}H_{984}B_7Br_{24}F_{28}N_{48}O_{144}Pd_{12}$ $[M - 17(BF_4)]^{17+}$ 1304.885, found 1305.205; *m/z* calcd for $C_{1200}H_{984}B_6Br_{24}F_{24}N_{48}O_{144}Pd_{12}$ $[M-18(BF_4)]^{18+}$ 1227.558, found 1227.567.

Crystal Parameters for ***L1***$\subset CBPQT^{4+}$ *(*$C_{38}H_{33}BrN_2O_6\subset C_{36}H_{32}F_{24}N_4P_4\cdot C_2H_3N$*).* Monoclinic, space group *C*2/*c* (No. 15), a = 24.6360(7) Å, b = 13.1360(3) Å, c = 48.4001(12) Å, β = 98.9838(17)°, V = 15 471.0(7) Å^3, Z = 8, T = 100.19 K, μ(Cu Kα) = 2.552 mm^{-1}, D_{calc} = 1.593 g/cm^3, 39 640 reflections measured (7.62 ≤ 2θ ≤ 122.318), 11 358 unique (R_{int} = 0.0540, R_{sigma} = 0.0471) which were used in all calculations. The final R_1 was 0.0508 ($I > 2\sigma(I)$) and wR_2 was 0.1227 (all data).

Crystal Parameters for ***Pd*$_{12}$*L1*$_{24}$**$\cdot$*24BF*$_4$ *(*$C_{492}H_{252}B_{24}Br_{24}N_{48}O_{24}F_{96}$ *and the Unmodeled DNP Groups).* Trigonal, space group *R*3, $a = b$ = 63.1380(3) Å, c = 41.6090(3) Å, V = 143647.9(17) Å^3, Z = 8, T = 293 K, μ(for λ = 0.750 Å) = 0.724 mm^{-1}, D_{calc} = 0.433 g/cm^3, 63 010 reflections measured (2.210 ≤ 2θ ≤ 33.250), 13 944 unique (R_{int} = 0.0736, R_{sigma} = 0.0489) which were used in all calculations. The final R_1 was 0.2139 ($I > 2\sigma(I)$) and wR_2 was 0.5207 (all data).

Molecular Mechanics. Energy-minimized geometries for the endohedral DNP threads of $\mathbf{Pd_{12}L1_{24}}^{24+}$, $\mathbf{Pd_{12}L2_{24}}^{24+}$, and $\mathbf{Pd_{12}L0_{12}L1_{12}}^{24+}$ were calculated in Hyperchem (Hypercube, Inc.) using the MM+ forcefield with a Polak−Ribiere conjugate gradient algorithm, a convergence limit of 0.001 kcal mol^{-1}, and a root-mean-square gradient of 0.001 kcal Å^{-1} mol^{-1}. The atoms of the crystallographically resolved ligand backbones of the coordination cages were fixed during these optimizations. Molecular graphics and analyses were performed with the UCSF Chimera package. Chimera is developed by the Resource for Biocomputing, Visualization, and Informatics at the University of California, San Francisco (supported by NIGMS P41-GM103311).[28]

■ ASSOCIATED CONTENT

Supporting Information

Synthetic procedures and characterization of new compounds, spectrophotometric titrations of **L1**$\subset$CBPQT^{4+}, ^{1}H and ^{13}C NMR spectra of $Pd_{12}L_{24}$ assemblies, ^{1}H DOSY NMR spectra, X-ray crystallographic details, mass spectra of $Pd_{12}L_{24}$ assemblies, Job plot of CBPQT$^{4+}\subset$**Pd$_{12}$L1$_{24}$**$^{24+}$, and ITC data. This material is available free of charge via the Internet at http://pubs.acs.org.

■ AUTHOR INFORMATION

Corresponding Authors

stoddart@northwestern.edu

mfujita@appchem.t.u-tokyo.ac.jp

Author Contributions

‡C.J.B. and D.F. contributed equally.

Notes

The authors declare no competing financial interest.

■ ACKNOWLEDGMENTS

This research was supported by Japan Science and Technology Agency (JST) Core Research for Evolutional Science and Technology (CREST) Program and Japan Society for the Promotion of Science (JSPS) Grants-in-Aid for Specially Promoted Research (24000009), as well as by the Joint Center of Excellence in Integrated Nano-Systems (JCIN) at King Abdulaziz City for Science and Technology (KACST) and Northwestern University (NU, Project 34-948). The synchrotron X-ray crystallography experiments were performed at SPring-8 and KEK. Travel and accommodation for our collaboration was supported by the University of Tokyo Global Center of Excellence (GCOE) "Chemistry Innovation through Cooperation of Science and Engineering" program, the Japan Society for the Promotion of Science (JSPS) Summer Program, and the National Science Foundation (NSF) East Asia and Pacific Summer Institutes (EAPSI) program under award no. 1316215. The authors thank Albert Fahrenbach for participation in the GCOE program; Subhadeep Basu, Ashish Basuray, Andrew Sue, Chuyang Cheng, and Margaret Schott for shipping compounds between our laboratories in Tokyo and Evanston; Aleksandr Bosoy for preparation of the TOC graphic; and Charlotte C. Stern and the personnel in the Integrated Molecular Structure Education and Research Center (IMSERC) at NU for assistance in the collection of X-ray crystallographic data and access to NMR instrumentation.

■ REFERENCES

(1) Yoshizawa, M.; Klosterman, J. K.; Fujita, M. *Angew. Chem., Int. Ed.* **2009**, *48*, 3418−3438.

(2) (a) MacGillivray, L. R.; Atwood, J. L. *Angew. Chem., Int. Ed.* **1999**, *38*, 1019−1034. (b) Liu, Y.; Hu, C.; Comotti, A.; Ward, M. D. *Science* **2011**, *333*, 436−440.

(3) (a) Cook, T. R.; Zheng, Y.-R.; Stang, P. J. *Chem. Rev.* **2013**, *113*, 734−777. (b) Dalgarno, S. J.; Power, N. P.; Atwood, J. L. *Coord. Chem. Rev.* **2008**, *252*, 825−841. (c) Sham, K.-C.; Yiu, S.-M.; Kwong, H.-L. *Inorg. Chem.* **2012**, *52*, 5648−5650.

(4) Harris, K.; Fujita, D.; Fujita, M. *Chem. Commun.* **2013**, *49*, 6703−6712.

(5) (a) Tominaga, M.; Suzuki, K.; Kawano, M.; Kusukawa, T.; Ozeki, T.; Shakamoto, S.; Yamaguchi, K.; Fujita, M. *Angew. Chem., Int. Ed.* **2004**, *43*, 5621−5625. (b) Gütz, C.; Hovorka, R.; Klein, C.; Jiang, Q.-Q.; Bannwarth, C.; Engeser, M.; Schmuck, C.; Assenmacher, W.; Mader, W.; Topić, F.; Rissanen, K.; Grimme, S.; Lützen, A. *Angew. Chem., Int. Ed.* **2014**, *53*, 1693−1698. (c) Jiang, F.; Wang, N.; Du, Z.; Wang, J.; Lan, Z.; Yang, R. *Chem.—Asian J.* **2012**, *7*, 2230−2234.

(6) (a) Sun, Q.-F.; Iwasa, J.; Ogawa, D.; Ishido, Y.; Sato, S.; Ozeki, T.; Sei, Y.; Yamaguchi, K.; Fujita, M. *Science* **2010**, *328*, 1144−1147. (b) Bunzen, J.; Iwasa, J.; Bonakdarzadeh, P.; Numata, E.; Rissanen, K.; Sato, S.; Fujita, M. *Angew. Chem., Int. Ed.* **2012**, *51*, 3161−3163.

(7) (a) Suzuki, K.; Sato, S.; Fujita, M. *Nature Chem.* **2010**, *2*, 25−29. (b) Takao, K.; Suzuki, K.; Ichijo, T.; Sato, S.; Asakura, H.; Teramura, K.; Kato, K.; Ohba, T.; Morita, T.; Fujita, M. *Angew. Chem., Int. Ed.* **2012**, *51*, 5893−5896. (c) Ichijo, T.; Sato, S.; Fujita, M. *J. Am. Chem. Soc.* **2013**, *135*, 6786−6789.

(8) Fujita, D.; Suzuki, K.; Sato, S.; Yagi-Utsumi, M.; Yamaguchi, Y.; Mizuno, N.; Kumasaka, T.; Takata, M.; Noda, M.; Uchiyama, S.; Kato, K.; Fujita, M. *Nature Commun.* **2012**, *3*, 1093−1097.

(9) (a) Murase, T.; Sato, S.; Fujita, M. *Angew. Chem., Int. Ed.* **2007**, *46*, 1083−1085. (b) Kikuchi, T.; Murase, T.; Sato, S.; Fujita, M. *Supramol. Chem.* **2008**, *20*, 81−94.

(10) Sun, Q.-F.; Sato, S.; Fujita, M. *Chem. Lett.* **2011**, *40*, 726−727.

(11) Sun, Q.-F.; Murase, T.; Sato, S.; Fujita, M. *Angew. Chem., Int. Ed.* **2011**, *50*, 10318−10321.

(12) Elemans, J.A.A.W.; Rowan, A. E.; Nolte, R. J. M. *J. Mater. Chem.* **2013**, *13*, 2661−2670.

(13) Cram, D. J. *Angew. Chem., Int. Ed. Engl.* **1988**, *27*, 1009−1020.

(14) (a) Coskun, A.; Spruell, J. M.; Barin, G.; Dichtel, W. R.; Flood, A. H.; Botros, Y. Y.; Stoddart, J. F. *Chem. Soc. Rev.* **2012**, *41*, 4827−4859. (b) Coskun, A.; Banaszak, M.; Astumian, R. D.; Stoddart, J. F.; Grzybowski, B. A. *Chem. Soc. Rev.* **2012**, *41*, 19−30. (c) Boyle, M. M.; Smaldone, R. A.; Whalley, A. C.; Ambrogio, M. W.; Botros, Y. Y.; Stoddart, J. F. *Chem. Sci.* **2011**, *2*, 204−210.

(15) (a) Odell, B.; Reddington, M. V.; Slawin, A. M. Z.; Spencer, N.; Stoddart, J. F.; Williams, D. J. *Angew. Chem., Int. Ed. Engl.* **1988**, *27*, 1547−1550. (b) Amabilino, D. B.; Anelli, P.-L.; Ashton, P. R.; Brown, G. R.; Córdova, E.; Godínez, L.; Hayes, W.; Kaifer, A. E.; Philp, D.; Slawin, A. M. Z.; Spencer, N.; Stoddart, J. F.; Tolley, M. S.; Williams, D. J. *J. Am. Chem. Soc.* **1995**, *117*, 11142−11170. (c) Asakawa, M.; Dehaen, W.; L'abbé, G.; Menzer, S.; Nouwen, J.; Raymo, F. M.; Stoddart, J. F.; Williams, D. J. *J. Org. Chem.* **1996**, *61*, 9591−9595.
(16) Bourgeois, J.-P.; Fujita, M.; Kawano, M.; Sakamoto, S.; Yamaguchi, K. *J. Am. Chem. Soc.* **2003**, *125*, 9260−9261.
(17) Catterall, W. A. *Annu. Rev. Biochem.* **1995**, *64*, 493−531.
(18) Tominaga, M.; Suzuki, K.; Murase, T.; Fujita, M. *J. Am. Chem. Soc.* **2005**, *127*, 11950−11951.
(19) Wiseman, T.; Williston, S.; Brandts, J. F.; Lin, L. N. *Anal. Biochem.* **1989**, *179*, 131−137.
(20) Connors, K. A. *Binding Constants*; Wiley: New York, 1987.
(21) Suzuki, K.; Kawano, M.; Sato, S.; Fujita, M. *J. Am. Chem. Soc.* **2007**, *129*, 10652−10653.
(22) Mecozzi, S.; Rebek, J., Jr. *Chem.—Eur. J.* **1998**, *4*, 1016−1022.
(23) Li, D.; Zhou, W.; Landskron, K.; Sato, S.; Kiely, C. J.; Fujita, M.; Liu, T. *Angew. Chem., Int. Ed.* **2011**, *50*, 5182−5187.
(24) Hmadeh, M.; Fahrenbach, A. C.; Basu, S.; Trabolsi, A.; Benítez, D.; Li, H.; Albrecht-Gary, A.-M.; Elhabiri, M.; Stoddart, J. F. *Chem.—Eur. J.* **2011**, *17*, 6076−6087.
(25) Turnbull, W. B; Daranas, A. H. *J. Am. Chem. Soc.* **2003**, *125*, 14859−14866.
(26) For examples of hierarchical host−host−guest assemblies, see: (a) Lützen, A.; Renslo, A. R.; Schalley, C. A.; O'Leary, B. M.; Rebek, J., Jr. *J. Am. Chem. Soc.* **1999**, *121*, 7455−7456. (b) Hardie, M. J.; Raston, C. L. *J. Chem. Soc., Dalton Trans.* **2000**, 2483−2492. (c) Masci, B.; Thury, P. *CrystEngComm* **2006**, *8*, 764−772. (d) Dalgarno, S. J.; Atwood, J. L.; Raston, C. L. *Chem. Commun.* **2006**, 4567−4574. (e) Dalgarno, S. J.; Fisher, J.; Raston, C. L. *Chem.—Eur. J.* **2006**, *12*, 2772−2777. (f) Shivanyuk, A. *J. Am. Chem. Soc.* **2007**, *129*, 14196−14199.
(27) For examples of gated binding, see: (a) Cram, D. J.; Tanner, M. E.; Knobler, C. B. *J. Am. Chem. Soc.* **1991**, *113*, 7717−7727. (b) Nakamura, K.; Houk, K. N. *J. Am. Chem. Soc.* **1995**, *117*, 1853−1854. (c) Houk, K. N.; Nakamura, K.; Sheu, C.; Keating, A. E. *Science* **1996**, *273*, 627−629. (d) Piatnitski, E. L.; Deshayes, K. D. *Angew. Chem., Int. Ed.* **1998**, *37*, 970−972. (e) Rieth, S.; Bao, X.; Wang, B.-Y.; Hadad, C. M.; Badjić, J. D. *J. Am. Chem. Soc.* **2010**, *132*, 773−776. (f) Rieth, S.; Hermann, K.; Wang, B.-Y.; Badjić, J. D. *Chem. Soc. Rev.* **2011**, *40*, 1609−1622. (g) Helgeson, R. C.; Hayden, A. E.; Houk, K. N. *J. Org. Chem.* **2010**, *75*, 570−575. (h) Wang, H.; Liu, F.; Helgeson, R. C.; Houk, K. N. *Angew. Chem., Int. Ed.* **2013**, *52*, 655−659.
(28) Pettersen, E. F.; Goddard, T. D.; Huang, C. C.; Couch, G. S.; Greenblatt, D. M.; Meng, E. C.; Ferrin, T. E. *J. Comput. Chem.* **2004**, *25*, 1605−1612.